

Fiber-optic voltage sensor based on a $\text{Bi}_{12}\text{TiO}_{20}$ crystal

Valery N. Filippov, Andrey N. Starodumov, Yuri O. Barmenkov, and Vadim V. Makarov

A fiber-optic voltage sensor based on the longitudinal Pockels effect in a $\text{Bi}_{12}\text{TiO}_{20}$ crystal is described. The use of a special backreflecting prism as a phase-retarding element is shown to improve the sensitivity and temperature stability of the sensor. A comparison between the temperature properties of the glass backreflecting prism and that of a quarter-wave plate is derived. The sensor demonstrates temperature stability of $\pm 1.5\%$ from -20°C to 60°C and sensitivity of 0.145% per 1 V_{rms} at 850 nm without the use of an additional temperature control channel. © 2000 Optical Society of America

OCIS codes: 060.2370, 230.2090, 230.5440, 260.1440.

1. Introduction

Fiber-optic voltage and electric field sensors have attracted much interest in recent years as an alternative to traditional measurements in electric power systems. These sensors are based on the Pockels effect and do not contain any conductive elements. As a result, the sensing head of the sensor introduces slight perturbations in the measured electric field. The first fiber-optic voltage sensor was demonstrated many years ago.^{1–6} There are two obstacles that prevent the application of these sensors in industry. First, their sensitivity is somewhat low. The typical sensitivity of voltage sensors with a longitudinal modulation is between 0.039% per 1 V_{rms} (Ref. 2) and 0.051% per 1 V_{rms} .¹ Second, the temperature stability of the entire sensor does not meet industrial requirements. In general, attention is paid to the temperature stability of crystal parameters.^{1,2,6,7–9} There are other optical elements inside the sensor, such as quarter-wave plates,¹⁰ that are sensitive to temperature changes. The changes in birefringence with temperature in this element causes the strong variation of the sensor's sensitivity.

We propose a new configuration of a fiber-optic voltage sensor, based on the $\text{Bi}_{12}\text{TiO}_{20}$ crystal. Instead of a quarter-wave plate we used a glass backreflecting prism as a phase-retarding element. By

using this prism, we demonstrated the good temperature stability of $\pm 1.5\%$ from -20°C to 60°C and excellent sensitivity without the use of an additional temperature control channel.

2. Basic Principle of the Sensor

The optical scheme of the sensor is shown in Fig. 1. The light from an 850-nm light-emitting diode is launched into the sensor through a multimode fiber ($300\text{--}320\ \mu\text{m}$) and Selfoc lens. The polarization state of the light after the addition of the polarizing prism is 45° to the axes of the electric field-induced birefringence of the crystal. When we applied an electric field, the original birefringence of the crystal became uniaxial because of the Pockels effect. The $5\text{ mm} \times 5\text{ mm} \times 2\text{ mm}$ crystal was aligned in such a way that the electric field and the optical path were normal to the (100) crystal plane.

The polarized light returned to the crystal after two reflections from the surface of the backreflecting prism. After the second pass through the crystal the beam meets the polarizing prism at the point where two orthogonal states of polarization separate into two channels. The analyzer converts the polarization modulation into intensity modulation in two channels. Both intensity-modulated beams were launched into the fibers by use of Selfoc lenses (Fig. 1).

The vertical axes of the reflecting prism and the polarizing prism are aligned at the angle of $45^\circ \pm \vartheta$, where ϑ is the angle of polarization rotation that is due to the optical activity of the crystal. The plus sign or minus sign changes according to the crystal modification (left-hand side or right-hand side rotation). On the other hand, this prism introduces a $\pi/2$ phase shift between the fast and the slow waves

The authors are with the Centro de Investigaciones en Optica, A.C., Loma del Bosque No. 115, Col. Lomas del Campestre, Apartado Postal 1-948, 37150 Leon, GTO, Mexico. The e-mail address for V. Filippov is valera@foton.cio.mx.

Received 9 March 1999; revised manuscript received 22 September 1999.

0003-6935/00/091389-05\$15.00/0

© 2000 Optical Society of America

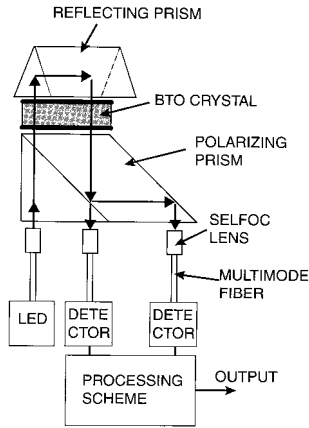


Fig. 1. Schematic of the sensor.

in the crystal, which permits one to use the best sensitivity of the sensor.¹¹

The angle of incidence and the refractive index of a prism¹² can be used to determine a phase shift between *S* and *P* polarizations based on total internal reflection. If one selects the correct angle of incidence and refractive index, it is possible to obtain a desirable phase shift between *S* and *P* polarizations. Note that the Fresnel rhombus, a well-known phase-shifting device, functions similarly.

To calculate the refractive index of the backreflecting prism we used the phase shift Δ between *S* and *P* polarizations on the glass-air interface of the backreflecting prism under total internal reflection¹²:

$$\tan(\Delta/2) = \frac{(n_1/n_0)[(n_0/n_1)^2 \sin^2 \varphi - 1]^{1/2}}{\sin \varphi \tan \varphi}, \quad (1)$$

where φ is the angle of incidence, n_1 and n_0 are the refractive indices of the air and glass prisms, respectively. By using Eq. (1) and $\varphi = \pi/4$, we calculated $n_1 = 1$, the refractive index of the backreflecting prism, as

$$n_0 = \left[\frac{2}{1 - \tan^2(\Delta/2)} \right]^{1/2}. \quad (2)$$

The phase shift Δ should equal $\pi/4$ to obtain the circular polarization of the beam after two consecutive reflections from surfaces of the prism. From this condition the refractive index of the prism n_0 was calculated to be 1.553773974. We used the BK-10 (Russian) glass¹³ with $n_0 = 1.56023$ at $\lambda = 863$ nm.

A. Sensitivity of the Sensor

Use of a backreflecting prism allows for an increase in sensitivity and improvement of the temperature stability of the sensor in comparison with the sensors reported in Refs. 1–6 and 7–9. The backreflecting prism has two important functions in the sensor. First, the prism is applied as a beam reflector in the double-pass scheme. The phase shift between fast and slow waves after the second pass through the crystal is doubled, resulting in the increase of sensi-

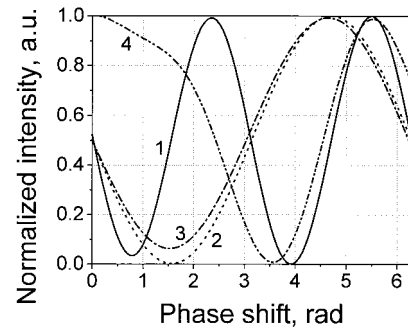


Fig. 2. Transfer function versus phase delay between fast and slow waves: 1, two-pass BTO sensor; 2, single-pass BTO sensor; 3, single-pass BSO sensor; 4, two-pass BSO-sensor.

tivity. Second, the reflective prism, as a phase-shifting element, is achromatic, i.e., the phase shift in the prism does not depend on wavelength, providing the maximum depth of modulation for all the spectral components of a laser source.

Below we present a detailed analysis of the advantages of the prism compared with a crystal quarter-wave plate. We begin with the sensitivity of the sensor. By use of the Jones matrix formalism, the transfer function of the sensor (Fig. 1) can be presented as

$$I = |P \times R(-45^\circ) \times C_{\text{ref}} \times R(45^\circ) \times R(-45^\circ - \vartheta) \times \text{PHASE} \times R(45^\circ + \vartheta) \times R(-45^\circ) \times C_{\text{dir}} \times R(45^\circ) \times E|^2, \quad (3)$$

where E is the Jones vector of light at the input of the crystal, $R(\dots)$ is the rotation matrix, C_{dir} is the Jones matrix of the BTO crystal for incident light, PHASE is the Jones matrix of the backreflecting prism, C_{ref} is the Jones matrix of the BTO crystal for backreflected light, and P is the Jones matrix of the analyzer.

With Eq. (3) we compared the sensitivity of the proposed two-pass sensor with that of the single-pass sensors, as described before in Refs. 1, 2, 4, 5, 8, and 9. The dependence of the transfer function on the phase shift between fast and slow waves in the BTO crystal for the two-pass sensor is shown in Fig. 2 (curve 1). Curve 2 in Fig. 2 presents the transfer function of the single-pass BTO sensor. As can be seen in the figure, the first minimum is achieved by curve 1 when the phase difference between fast and slow waves is equal to 0.817 rad; whereas the first minimum of curve 2 corresponds to a phase difference of 1.571 rad. Thus, the sensitivity of the two-pass sensor is approximately twice that of the single-pass sensor.

We have also compared the sensor sensitivity for two crystals: BSO ($\text{Bi}_{12}\text{SiO}_{20}$) and BTO. The BSO crystal has the high value of the electro-optic constant r_{41} and is readily available. The BSO has a high intrinsic optical activity ($11.5^\circ/\text{mm}$). The BTO crystal has the same value as the electro-optic constant r_{41} , but its optical activity is much less ($1.5^\circ/\text{mm}$). The transfer functions of the BSO-based

single-pass (curve 3) and double-pass (curve 4) sensors are shown in Fig. 2. We assume that the thickness of the crystal is 2 mm. As follows from our calculations, the sensitivity of the single-pass sensor (Fig. 2, curves 2 and 3) changes slightly during optical activity for both types of crystal. However, for double-pass configuration the sensitivity of the BSO-based sensor decreases significantly compared with the BTO-based sensor. Thus, the low optical activity of the BTO crystal makes it preferable for the double-pass configuration.

A comparison of achromatism of phase-shifting elements. In general, a broadband laser diode is used in sensors as a source of optical radiation, providing suppression of a modal noise at the output of multi-mode optical fibers. The typical spectral bandwidth of the diodes is 50–80 nm. The phase delay between the fast and the slow waves in a crystal phase plate is given by

$$\Phi_{\text{plate}} = \frac{2\pi\Delta nL}{\lambda}, \quad (4)$$

where Δn is the difference between the refractive index of the fast and slow axes, L is the thickness of the plate, and λ is the wavelength in the spectrum center of the laser diode.

As can be seen from Eq. (4), the phase shift changes with wavelength, resulting in different phase conditions for the different parts of the laser diode spectrum. Inasmuch as the $\pi/2$ phase shift at the center of the spectrum corresponds to the maximum modulation depth, the wavelengths at the wings of the spectrum with a phase shift that differs from $\pi/2$ are modulated with less efficiency, leading to reduction of the sensor's sensitivity (or the modulation depth).

We now compare the wavelength dependence of the phase shift in a crystalline phase plate and a reflective prism. The variation of the phase shift as a function of wavelength in the N th order phase plate can be written as

$$\delta\Phi_{\text{plate}} = \frac{2\pi\Delta nNL}{\lambda} \frac{\delta\lambda}{\lambda} = \Phi_{0\text{plate}}N \frac{\delta\lambda}{\lambda}. \quad (5)$$

By use of Eq. (5), the relative change of a phase delay is given by

$$\frac{\delta\Phi_{\text{plate}}}{\Phi_{0\text{plate}}} = N \frac{\delta\lambda}{\lambda}. \quad (6)$$

Thus, the relative change of a phase delay is proportional to the relative change of wavelength and to the order of a phase plate. For the relative phase change of 1% (a phase shift of approximately 1°) in the zero-order plate (850-nm wavelength), the spectral range corresponding to the phase variation within 1% is 8.5 nm. However, for the quarter-wave plate of the order of 28.25, this range is only 0.3 nm, resulting in less efficient modulation for wavelengths at the wings of the spectrum.

In the backreflecting prism a phase delay between

S and P polarizations can be calculated from Eq. (2) as

$$\Phi_{\text{prism}} = 4a \tan \sqrt{1 - (2/n^2)}. \quad (7)$$

When we use Eq. (7), a phase delay variation can be given by

$$\delta\Phi_{\text{prism}} = \frac{d\Phi_{\text{prism}}}{dn} \frac{dn}{d\lambda} \delta\lambda = -\frac{4}{(n^2 - 1)\sqrt{n^2 - 2}} \frac{dn}{d\lambda} \delta\lambda. \quad (8)$$

When we substituted $n = 1.56023$ and $dn/d\lambda = 1.6632 \times 10^{-5} \text{ nm}^{-1}$ into Eq. (8),¹³ we finally obtained

$$\delta\Phi = 7.047 \times 10^{-5} \delta\lambda. \quad (9)$$

For $\delta\lambda = 80 \text{ nm}$ the phase changes between S and P polarizations is only 0.3° . Thus, the phase shift in a backreflecting prism is similar for all the spectral components of a laser diode. As a result, all the spectral components will be modulated with the maximum depth of modulation, providing the best sensitivity of the sensor.

B. Reduction of Temperature Sensitivity

We have compared the temperature sensitivity of the proposed sensor with that of the sensors with quarter-wave plates.^{1–5,8–10} The temperature sensitivity of a phase plate is well known.^{7,14} We consider the quartz-made quarter-wave plate of zero order. The thickness (L) of this plate is 24 μm at 850-nm wavelength. The optical phase shift in the phase plate caused by temperature changes is given by

$$\Delta\Phi_{\text{plate}} = 2\pi\Delta nL\gamma\Delta T/\lambda, \quad (10)$$

where $\Delta n = 0.00885$ is the quartz birefringence at $\lambda = 850 \text{ nm}$, $\gamma = 1.4 \times 10^{-4} \text{ }^\circ\text{C}^{-1}$ is the constant that determines the changes of birefringence with temperature,⁷ and $\Delta T = 100 \text{ }^\circ\text{C}$ is the temperature range. Note that we neglected thermal expansion in Eq. (10).

As follows from Eq. (10), the temperature changes greater than $100 \text{ }^\circ\text{C}$ cause the additional phase retardance of approximately 1.26° in the zero-order phase plate. The low-order phase plates are not generally used because of fabrication difficulties. The high-order phase plates are much less stable

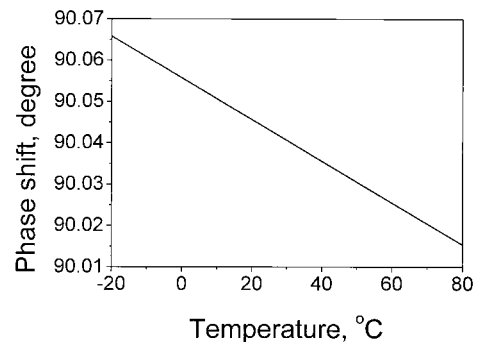


Fig. 3. Phase shift between S and P polarizations that is due to reflections in the prism as a function of temperature.

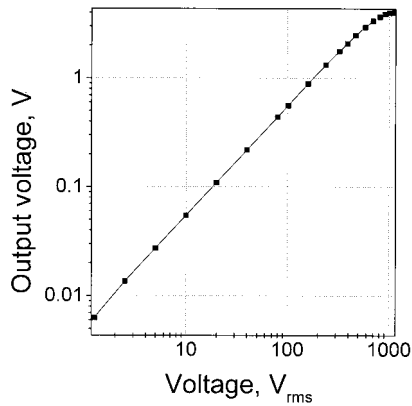


Fig. 4. Output voltage of the sensor versus applied voltage amplitude with a frequency of 50 Hz.

compared with low-order phase retarders. For example, the phase shift between fast and slow waves in the quartz-made quarter-wave plate¹⁴ of the order of $N = 28.25$ (thickness of 1.973 mm, $\lambda = 633$ nm) changes 1.03° with a temperature increase of 1°C . Temperature changes greater than 100°C would lead to a phase retardance of 103° .

We now consider the temperature stability of a glass backreflecting prism. The phase shift between S and P polarizations after two reflections is given by Eq. (7). The temperature stability of the prism depends on temperature properties of the glass refractive index. The temperature constant of BK-10 glass is $2 \times 10^{-6} \text{ }^\circ\text{C}^{-1}$.¹³ The dependence of the phase shift between S and P polarizations after two reflections in the prism as a function of temperature is shown in Fig. 3. As can be seen in Fig. 3, the phase shift caused by temperature changes over a range of 100°C is only 0.05° . Thus, a backreflecting prism as a phase retarder is at least 20 times more stable than a zero-order quartz-made quarter-wave plate.

3. Experiment

We experimentally investigated the sensitivity and temperature stability of the sensor. Figure 4 shows the output signal of the sensor's processing unit as a

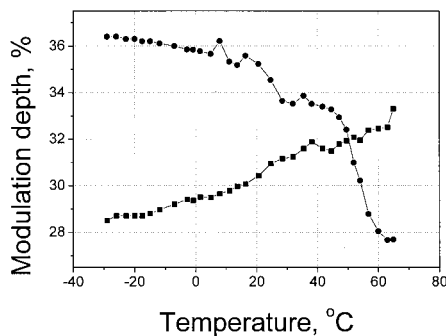


Fig. 5. Drift of sensitivity for different channels of the sensor with an applied voltage amplitude of $220 \text{ V}_{\text{rms}}$ and a frequency of 400 Hz.

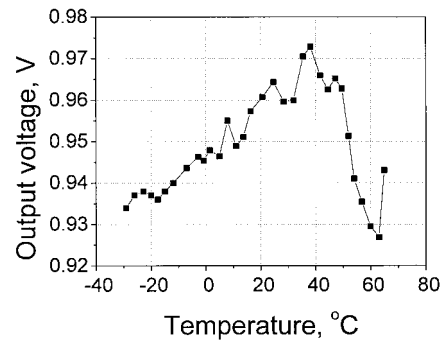


Fig. 6. Dependence of the output voltage of the sensor as a function of temperature with an applied voltage amplitude of $220 \text{ V}_{\text{rms}}$ and a frequency of 400 Hz.

function of applied voltage (50 Hz). As follows from Fig. 4, the dependence of the sensor output signal on applied voltage becomes nonlinear for amplitudes of approximately $1000 \text{ V}_{\text{rms}}$. It is directly related to the nonlinear behavior of the sensor transfer function (see Fig. 2, curve 1) and to the high sensitivity of the sensor (0.145% per 1 V_{rms}). The minimum detected voltage (3-dB signal-to-noise ratio, frequency band of 1.5–25000 Hz) was $0.35 \text{ V}_{\text{rms}}$.

Figure 5 shows the temperature dependence of the modulation depth for different channels of the sensor. As can be seen from Fig. 5, the modulation depth for different channels of the sensor varies in opposite directions with temperature. Such behavior can be explained by the complex mechanical structure of the sensor. All the elements of the sensor (BTO crystal, the glass prisms, Selfoc lens) are glued together so that the sensor represents a single unit. The significant temperature change (from -20°C to 60°C) causes the appearance of mechanical stress in the sensor head. The intrinsic mechanical stress, in turn, results in additional linear birefringence in the crystal because of the photoelastic effect. The temperature-induced drift of the additional linear birefringence leads to the changes of the optical power in each channel, resulting in changes of the sensor sensitivity.

To improve the temperature stability and signal-to-noise ratio we processed the output signals from both channels in the electronic block with specially chosen weights. As a result, the combined signal demonstrated better stability. The temperature dependence of the combined signal from two channels is shown in Fig. 6. The temperature stability of the sensor output signal was measured to be approximately $\pm 1.5\%$ in the range from -20°C to 60°C .

4. Conclusion

We have demonstrated a fiber-optic electric voltage sensor based on a BTO crystal with an inherently high temperature stability. A special backreflecting prism was used as the phase-retarding element as a substitute for temperature-sensitive birefringent elements in the optical scheme. The sensor demonstrates temperature stability of $\pm 1.5\%$ from

–20 °C to 60 °C and sensitivity of 0.145% per 1 V_{rms} at 850 nm without the use of a temperature control channel.

References

1. Y. Hamasaki, H. Gotoh, M. Katoh, and S. Takeuchi, "OPSEF: an optical sensor for measurement of high electric field intensity," *Electron. Lett.* **16**, 406–407 (1980).
2. Y. Kuhara, Y. Hamasaki, A. Kawakami, Y. Murakami, M. Tatsumi, H. Takimoto, K. Tada, and T. Mitsui, "BSO/fibre-optic voltmeter with excellent temperature stability," *Electron. Lett.* **18**, 1055–1056 (1982).
3. J. P. Dakin and M. C. Holliday, "A passive all-dielectric field probe for R.F. measurement using the electro-optic effect," in *Fiber Optics '84*, J. M. Tait, ed., *Proc. SPIE* **468**, 237–240 (1984).
4. K. Kyuma, S. Tai, M. Nunoshita, N. Mikami, and Y. Ida, "Fiber-optic current and voltage sensors using a Bi₁₂GeO₂₀ single crystal," *J. Lightwave Technol.* **LT-1**, 93–97 (1983).
5. M. Norimatsu and M. Shirasaki, "Bi₁₂SiO₂₀ crystal application for voltage sensor in optical fibers," *Ferroelectrics* **75**, 189–196 (1987).
6. A. H. Rose and G. W. Day, "Optical fiber voltage sensors for broad temperature ranges," in *Fiber Optic Components and Reliability*, P. M. Kopera and D. K. Paul, eds., *Proc. SPIE* **1580**, 95–103 (1992).
7. J. Niewisch, P. Menke, P. Krammer, and T. Bosselmann, "Temperature drift compensation of a potential transformer using a BSO Pockels cell," in *Proceedings of the 11th International Conference on Optical Fiber Sensors: Advanced Sensing Photonics* 21–24 May 1996, Sapporo, Japan, (Japan Society of Applied Physics, Tokyo, 1996), pp. 152–155.
8. A. Koch, C. Helmig, and H. Senftleben, "Experimental studies on a temperature compensation for optical voltage sensing," in *Optical Fiber Sensors*, Vol. 16 of OSA 1997 Technical Digest Series (Optical Society of America, Washington, D.C., 1997), pp. 257–260.
9. T. Bosselmann, "Magneto- and electrooptic transformers meet expectations of power industry," in *Optical Fiber Sensors*, Vol. 16 of OSA 1997 Technical Digest Series (Optical Society of America, Washington, D.C., 1997), pp. 771–774.
10. P. D. Hale and G. W. Day, "Stability of birefringent linear retarders (waveplates)," *Appl. Opt.* **27**, 5146–5153 (1988).
11. A. Yariv and P. Yeh, *Optical Waves in Crystals* (Wiley, New York, 1984).
12. R. M. A. Azzam and N. M. Bashara, *Ellipsometry and Polarized Light* (North-Holland, Amsterdam, 1977).
13. Industrial Standard of the USSR: GOST No. 13659-78, BK-10 Glass, (Edition of Standards, Moscow, 1981), in Russian.
14. W. G. Driscoll and W. Vaughan, eds., *Handbook of Optics* (McGraw-Hill, New York, 1978).